

Article

Influence of Moisture in Quartzite on the Lining Properties and Efficiency of Industrial-Frequency Induction Crucible Furnaces

Viktor Alekseevich Kukartsev ¹, Aleksandr Ivanovich Cherepanov ¹, Vladislav Viktorovich Kukartsev ^{2,3,4}, Vadim Sergeevich Tynchenko ^{4,5,6,*} , Sergei Olegovich Kurashkin ^{4,5,7,*} , Valeriya Valerievna Tynchenko ^{8,9}, Roman Borisovich Sergienko ¹⁰, Kirill Aleksandrovich Bashmur ⁶ , Andrei Anatolevich Boyko ^{4,6,11} and Vladimir Viktorovich Bukhtoyarov ^{4,6} 

- ¹ Department of Materials Science and Materials Processing Technology, Polytechnical Institute, Siberian Federal University, 660041 Krasnoyarsk, Russia
 - ² Department of Informatics, Institute of Space and Information Technologies, Siberian Federal University, 660041 Krasnoyarsk, Russia
 - ³ Department of Information Economic Systems, Institute of Engineering and Economics, Reshetnev Siberian State University of Science and Technology, 660037 Krasnoyarsk, Russia
 - ⁴ Digital Material Science: New Materials and Technologies, Bauman Moscow State Technical University, 105005 Moscow, Russia
 - ⁵ Information-Control Systems Department, Institute of Computer Science and Telecommunications, Reshetnev Siberian State University of Science and Technology, 660037 Krasnoyarsk, Russia
 - ⁶ Department of Technological Machines and Equipment of Oil and Gas Complex, School of Petroleum and Natural Gas Engineering, Siberian Federal University, 660041 Krasnoyarsk, Russia
 - ⁷ Laboratory of Biofuel Compositions, Siberian Federal University, 660041 Krasnoyarsk, Russia
 - ⁸ Department of Computer Science, Institute of Space and Information Technologies, Siberian Federal University, 660041 Krasnoyarsk, Russia
 - ⁹ Department of Computer Science and Computer Engineering, Institute of Computer Science and Telecommunications, Reshetnev Siberian State University of Science and Technology, 660037 Krasnoyarsk, Russia
 - ¹⁰ Machine Learning Department, Gini GmbH, 80339 Munich, Germany
 - ¹¹ Department of Management, Reshetnev Siberian State University of Science and Technology, 660037 Krasnoyarsk, Russia
- * Correspondence: vadimond@mail.ru (V.S.T.); scorpion_ser@mail.ru (S.O.K.); Tel.: +79-50-973-0264 (V.S.T.)



Citation: Kukartsev, V.A.; Cherepanov, A.I.; Kukartsev, V.V.; Tynchenko, V.S.; Kurashkin, S.O.; Tynchenko, V.V.; Sergienko, R.B.; Bashmur, K.A.; Boyko, A.A.; Bukhtoyarov, V.V. Influence of Moisture in Quartzite on the Lining Properties and Efficiency of Industrial-Frequency Induction Crucible Furnaces. *Metals* **2022**, *12*, 1515. <https://doi.org/10.3390/met12091515>

Academic Editor: Mark E. Schlesinger

Received: 30 July 2022

Accepted: 12 September 2022

Published: 13 September 2022

Publisher's Note: MDPI stays neutral with regard to jurisdictional claims in published maps and institutional affiliations.



Copyright: © 2022 by the authors. Licensee MDPI, Basel, Switzerland. This article is an open access article distributed under the terms and conditions of the Creative Commons Attribution (CC BY) license (<https://creativecommons.org/licenses/by/4.0/>).

Abstract: The main purpose of industrial frequency induction crucible smelters (IGM) is the smelting of synthetic cast iron, using metal filling scrap in the amount of 30–35%, at a temperature not exceeding 1450 °C. The basis of the lining used is quartzite, which undergoes polymorphic transformations in the pre-treatment process to form tridimite. The efficiency of using these furnaces is significantly increased when using a metal casting consisting of a single steel scrap, but for this purpose, the melting mode has to be raised to 1550–1600 °C, which will reduce the resistance of the lining. The structural transformation of quartzite is strongly influenced by the state of water in it. In this work, studies have been carried out for changes in the water condition in the quartzite of the brand PCMVI-3 under the action of temperatures of 200–1550 °C. The Shimadzu XRF-1800 spectrometer established the actual chemical composition of the investigated quartzite and found that the amount of impurities in it is 0.66%. A derivative study of STA 449 F1 Jupiter found two endothermic effects. The first, at 170 °C, relates to the loss of adsorbed water. The second, at a temperature of 570 °C, passes without the loss of mass of the sample, and it is accompanied by the beginning of the process of the destruction of point defects in the form of Al-OH groupings. From a temperature of 620–630 °C, no mass changes associated with water removal were detected. The BRUKER D8 ADVANCE diffractometer investigated phase changes during the removal of moisture from the quartzite at temperatures of 200 and 800 °C and subsequent cooling and then during the heating used to sinter the lining. As a result, it has been established that the sheet in which the quartzite contains only chemically bound moisture, after sintering, turns into cristobalite and provides a more stable exposure to sudden temperature changes. This makes it possible to use up to 90% of the steel scrap in metal filling, which increases the efficiency of the melting furnace and the production of castings in general.

Keywords: derivative; durability; efficiency; induction furnace; innovation; lining resistance; melting modes; moisture condition in quartzite; technology innovation; synthetic cast iron

1. Introduction

The manufacturing of castings is the most common process of forming part blanks due to its low cost and comprehensive application. It makes it possible to obtain blanks with dimensions as close as possible to the profile of the future part and to provide the necessary requirements for mechanical, physical, technical and special properties specified in the technical conditions [1]. This process can be applied to both individual and mass production. Different alloys can be used for castings. Figure 1 presents the data for the used alloys and the smelting equipment for their smelting in Russia in 2020 [2].

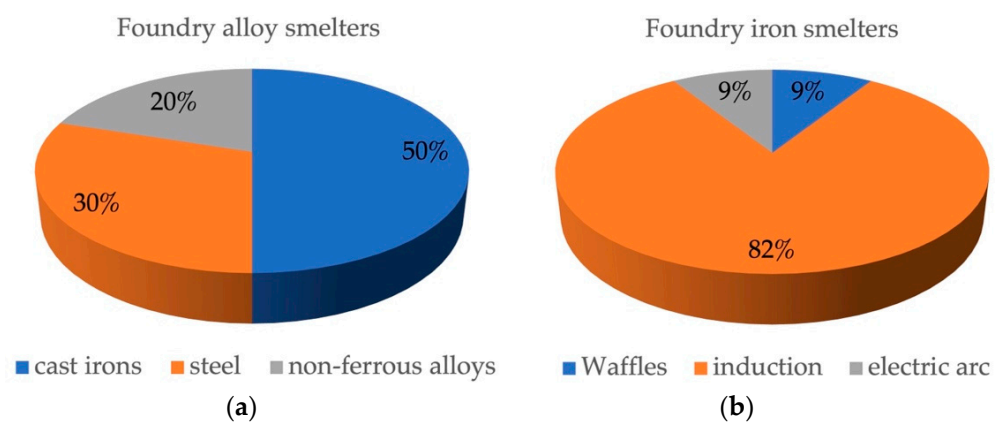


Figure 1. Structure of lost foundry alloys: (a)—foundry alloy smelters, (b)—foundry iron smelters.

Thus, in the production of castings, cast iron is the most common alloy, and for its smelting, induction furnaces are the most common. Of the total number of induction crucible furnaces, about 18% are high-frequency induction furnaces designed for the smelting of alloy steels and medium-frequency furnaces that can be used for smelting any alloys.

Industrial frequency induction crucible furnaces (IGS) have been in use since the 1950s [3–6]. They were intended for the smelting of synthetic cast iron, using steel scrap in the form of sheet trimming, shavings and other small-volume metal waste. This makes it possible to smelt waste at the place of its formation and provides a reduction in the cost of lost cast iron by 25–39% compared to cast iron of secondary melting [7–9]. This is particularly relevant in the current context, where all countries are facing the effects of the pandemic and the ensuing energy crisis [10].

Melting temperatures depend on the amount of steel scrap used in metal filling and the type of lining materials used. For this reason, the furnace’s designers limited the use of scrap to 30–35%, which ensured that the furnace could operate at a melting point of no more than 1450 °C and allowed for the use of a quartzite-based acid lining, as the cheapest option. The practice of operating the furnaces has shown the high resistance of this lining: 300–350 melts.

Details of the metal balance from gray iron smelting, which can be formed in induction furnaces, are given in Table 1.

Table 1. Balance of induction furnace metal in Russia.

Name	Amount (%)	
	Business Averages	Achieved in Some Industries
Shelf life	64.6	82.2
Rejects	2.3	2.9
Ungar	2	2
Sprues and arrived	29.5	8.9
Irretrievable losses	1.6	2
Plums and scrap	-	2
Result	100	100

Thus, the number of returns can range from $2.9 + 8.9 + 2 = 13.8\%$ to $2.3 + 29.5 = 31.8\%$.

The scrap metal required to produce a chemical composition corresponding to cast iron of GI20 (A48-30B in USA) is presented in Table 2.

Table 2. Composition of metal scrap for different amounts of steel content.

Metal Content	Content of Constituents (%)	
	Traditional Composition	Efficiency-Enhancing
Zumpf (liquid residue)	30–33	10–20
Production return	15–32	0
Cast iron removable, and cast iron scrap	10–15	0
Steel scrap	25–30	78–88
Ferromanganese/ferrosilicon	0.5–1	1–1.5
Carburizer	0.5–0.6	1–2
Indicative cost (thousands of rubles)	39.1	22.9

Traditional synthetic iron smelting technology requires the presence of a liquid residue (bog) after the discharge of finished melting (30–35%) and, following the first variant of metal filling, the use of return (31.8%) and steel scrap with the necessary ferroalloys. The absence of metal filling (the second variant) is due to the fact that it is necessary for use in the sintering process of the newly manufactured lining. The return is accumulated, shredded and loaded inside the template after the lining mixture is finished. The sintering process is produced only with cast iron, which ensures the necessary temperature conditions.

The smelting process requires a power reserve, allowing one to raise the temperature to 1550 °C for such technological operations as the process of carburization when using steel scrap, alloying during the smelting of special cast iron, the implementation of temperature exposure during the end of the sintering process of the new lining and the possibility of using a large amount of lightweight scrap and return. For this reason, the designers chose a power system that would allow for a more complete separation of power in the heated metal under different operating modes. Thus, in the design of the furnace, a transformer is applied, which has a constant power on the first four or five voltage stages, with a certain reserve of power, because when operating at low-voltage stages, at the rated power, the current of the transformer will be greater than that at the rated voltage. The final refining of the melt, with a fully filled crucible, requires a high temperature. For this reason, the equivalent of the active resistance of the “inductor-garden” system $R_{equiv} = U_i^2 / R_i$ is significantly reduced, and the total capacity of the furnace must increase. An illustration of this is the graph of the dependence of the active resistance on the metal filling of the crucible, as shown in Figure 2.

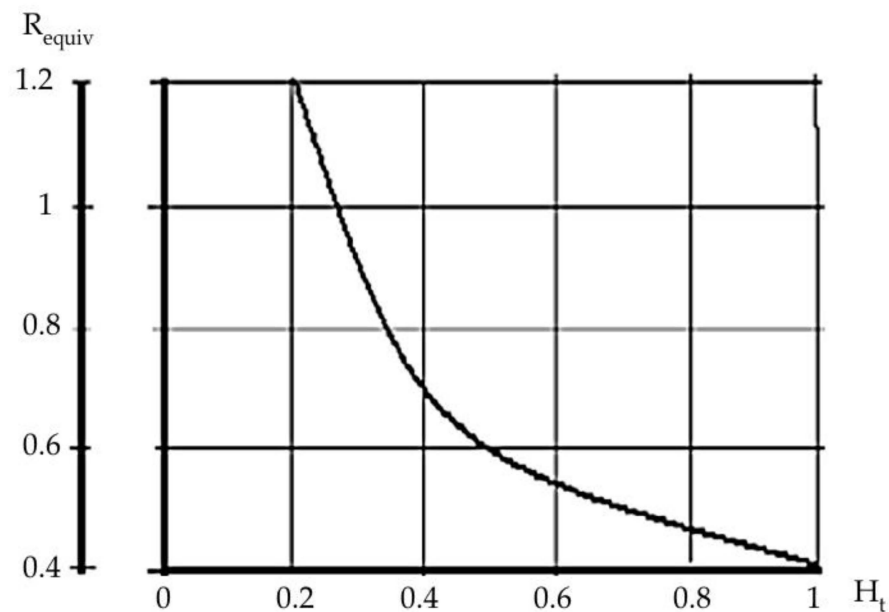


Figure 2. Graph of the dependence of active resistance R_{equiv} on the size of the fill of the crucible in height H_t [11].

It is shown that, for the furnace, the capacity is 40t when the crucible is fully filled with $R_{equiv} = 0.4$; when filled with 0.2 R_{equiv} , the height increases to 1.2. For this reason, the constructor has a power reserve of 15–20% [9].

Thus, the design of the furnace allows for the smelting of synthetic cast iron in conditions above 1450 °C, but the efficiency of its operation depends on the durability of the lining. Finding solutions to improve the life cycle of the smelter is one of the objectives of increasing production efficiency [11].

For foundries (enterprises), it is only possible to gain a market for their products by achieving a greater profitability and efficiency of the product through the use of advanced technologies. First of all, this is achieved by saving on production costs, such as reducing downtime and increasing the performance of major equipment.

The induction crucible is the basis of the foundry's production capacity, so it significantly affects labor productivity and profitability. For this reason, the creation of conditions that ensure an increase in the reliability of the operation of smelting equipment is the most important task.

As early as the 1980s, it was found that the constant use of melting temperatures of more than 1450 °C leads to a reduction in the resistance of the acid lining from 300–350 to 180–200 melts. For this reason, the downtime of the smelting furnace associated with the construction of the number of torches is increasing. It takes 2.5–3 days for the IGS-1 melting furnace to be turned over (one ton capacity) from the start of the shutdown to the discharge of the first full bucket. Therefore, the increase in the number of faults leads not only to an increase in downtime and material costs but also to an increase in the consumption of electricity for drying quartzite. All this reduces the production efficiency and affects competitiveness, as the market requires not only quality but also attractive price castings.

Repeated attempts have been made to improve the properties of the acid lining when smelting an alloy for a metal filling that requires a temperature of more than 1450 °C. Additives from a mixture of calcium, iron and sodium, phosphorus-containing additives, a special fritta fused from a mixture of silica and sodium oxide or silica with iron oxides and calcium, Tridimate grinder in the form of the fine grinding of triimized dynas or 30% corundum additives have been used.

In 1991, a refractory mass containing fine chromium oxide as a chrome-containing additive and an additional sodium silicate and a mullithic roonde mortar were proposed [12].

In 1997, Pivinsky Yu.E. proposed a silica-neutral refractory mass based on quartzite or quartz aggregate and astringent [13]. Svatkin A.S., in 2008, proposed the addition of mineralizers [14].

High-temperature additives in the form of ZrO_2 , Cr_2O_3 , chromoglobulin slag and chromite have also been proposed. However, they have not been commercially applied. In other countries, emphasis was placed on the use of liner materials in the form of finished products.

In addition, the question of price cannot be ignored. Corundum Mass is RUB 70 per 1 kg, Corundum Lining Mass Coral CXL is RUB 500 per 1 kg, Heat-Resistant Induction Furnaces for Smelting Alloy Steel and Cast Iron at Temperatures up to 1800 C are RUB 180 per 1 kg, Mass Dry Acid Cyte Astro FSBOND 984 is RUB 14 per 1 kg and quartzite ground PCMVI 2 is RUB 11 per 1 kg.

Thus, increasing the resistance of the quartzite-based acid lining by changing its properties is the most advantageous way to increase the efficiency of operation of the induction furnace.

For this reason, this paper focuses on the role of the moisture state in the original quartzite on the lining stability at smelting temperatures above 1450 °C.

The composition of the properties of quartzite depends on the number and composition of mineral phases—minerals—satellites, minerals—inclusions, gas—liquid inclusions (GLI), gases and vapors absorbed by the surface and mechanical disperse particles in cracks, voids and on the surface thereof. To produce a quartzite with a high SiO_2 content and a minimum number of impurities, its manufacturers use a wet enrichment method that includes washing, scrubbing, gravity, magnetic separation and flotation operations. This technology avoids dust formation during grinding and the pollution of the atmosphere causing silicosis, so quartzite is moistened to 2–3%. For this reason, [15–18] reflects that the use of wet quartzite for the preparation of the lining of tiger induction furnaces requires additional drying to a moisture content of 0.3%, with the further production of tridimite and cristobalite phases.

The work [19] concluded that the formation of these phases depends not only on the chemical purity of the quartzite and the mineralizers used but also on the number of structural impurities and volatile components, of which the main ones are water (up to 92%) and carbon dioxide (up to 8%). The works [20–25] show that these components are in trace amounts in different hydrogen-containing groupings. The degree of crystallization of quartzite depends on a number of factors, including the number and composition of the GLI itself; this is reflected in the works [26–28]. The works [29–32] establish the conditions for the release of hydroxyl groups (OH) that contribute to the formation of the water molecule, which leads to the restructuring and ordering of the quartzite structure.

The process of removing film moisture is described in the works [33–36]; it occurs at a temperature of 940–950 °C and causes particle convergence, but in comparison with the removal of mechanically connected water, it is rather insignificant. In the works [37,38], it is established that point defects in the form of Al-OH groups begin to break down at 600 °C and are completely removed at 1100 °C, and their removal does not cause shrinkage.

The use of temperature melting modes above 1450 °C requires the use of a higher temperature phase of quartzite, which is cristobalite.

Tridimite is stable at 870–1470 °C, has a density of 2.23 g/cm³ and has a hardness of 6.5 units on the Mohs scale.

Cristobalite cubic is stable at a temperature of 1470–1715 °C, has a hardness of 7.25 and has a density of 2.27 g/cm³. The sintered layer, with a hardness that is 11.5% higher, is therefore more stable at melting temperatures above 1450 °C, as it is better able to withstand the active mixing of the surface layers of the melt in contact with it.

The novelty of the work is thus as follows:

1. Studies have found that the minimum amount of GLI leads to trisimite, and the maximum is cristobalite, which is detected after its temperature treatment during drying and the further exposure to temperature melting conditions;

2. Impurities detected by the X-ray fluorescent wvdispersion spectrometer Shimadzu XRF-1800 in the amount of 1.149% are found not to be mineralizers, but despite this, when using a traditional proclomator at 800 °C, the phase transformation of the quartzite remains unchanged. At 600 °C, a polymorphic transformation occurs, which results in the emergence of a tridimite elementary cell, and cristobalite cells appear only at 1550 °C;
3. Studies using the derivative STA 449 F1 Jupiter showed that free water is removed from the quartzite at temperatures of 170–200 °C. This is characterized by the first endoeffect derivative and refers to the loss of adsorbed (physically bound) water. The second endoeffect is observed at a temperature of 570 °C and relates to polymorphic transformation leading to alpha-quartz phase formation in beta-quartz. It is accompanied by the beginning of the process of removing chemically bound water and is not accompanied by a change in mass;
4. Moisture has been found to act as a mineralizer, and its condition influences the formation of specific phases. This assumption was made in the work [39]. Temperature treatment at 800 °C results in the complete removal of free water and a significant amount of chemically bonded water, including GLL, which reduces the efficiency of the structural conversion of quartzite to cristobalite and promotes the formation of tridymite;
5. Drying at 200 °C results only in the removal of free water and contributes to the process of crystallization. Cristobalite begins to appear at 870 °C; the tridimite phase is not detected even at 1550 °C;
6. It has been determined that tridymite, within the temperature range of 1000–1550 °C (these are the working temperatures at the smelting of synthetic cast iron from metal filling consisting of up to 90% steel scrap), allows for volume changes in the limit of 9% and cristobalite in the limit of 15%.

Thus, the lining in which the quartzite contains only chemically bonded moisture, after the sintering of the lining, is converted to cristobalite and provides a more stable exposure to sudden temperature changes. This makes it possible to apply the melting temperatures required for use in metal processing up to 90% of scrap steel, which increases the efficiency of the melting furnace and the production of castings in general. So, for the IGT-1 furnace, the use of this scrap metal only reduces the cost for the purchase of bulk materials by 61–68.8%.

2. Materials and Methods

2.1. Formulation of the Problem

Practice has found that the stability of quartzite lining at a temperature of more than 1450 °C significantly decreases. Thus, if the resistance of the crucible 12t furnace from the Pervoural quartzite during the melting and overheating of the cast iron up to 1450 °C reaches 320 swimwear (4 months and 1 week), then, with the increase in working modes of smelting up to 1550 °C, it decreases to 180–250 melts [40].

Thus, to increase production efficiency, the problem of maintaining the resistance of the lining becomes essential. The high durability of the traditional acid quartzite-based lining was ensured by the fact that, after sintering, it formed three layers: sintered, half-baked and untreated (Figure 3) [41].

In the process of the operation of the furnace, all these zones are reborn, there is wear of the lining and, eventually, there is a need to replace it after 300–350 melts, but this is only if the melting mode is not 1450 °C.

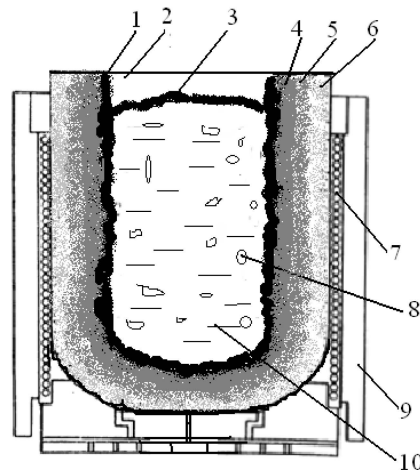


Figure 3. Diagram of the location of quartzite lining areas in the IRT furnace: 1—coated sintered lining layer; 2—gas phase on the melt surface; 3—liquid slag on the melt surface; 4—sintered layer; 5—semi-welded layer; 6—layer of unsteady mass (buffer); 7—inductor; 8—gas contained in the melt itself; 9—furnace housing; 10—melt.

Quartzite is still the most common material for making fireproof materials. Its active use began in the second half of the 18th century for the production of dyno products used in the lining of various heating and smelting furnaces [42–45]. It has been shown that the best properties are acquired by Dinas, in which the main amount of quartz has been transformed into tridymite under the influence of temperature, retaining a constant volume at 840–1470 °C for a long time and thereby ensuring the high resistance of the lining. The active use of quartzite-based acid lining for induction stoves began in the second half of the last century and persists to this day, as its price is below the basic and neutral by a factor of 4–6.

The composition of quartzite depends on the number and composition of mineral phases—minerals-satellites, minerals-inclusions, gas-liquid inclusions (GLI), gases and vapors absorbed by the surface and mechanical dispersion particles in cracks, voids and on the surface. To produce a quartzite with a high SiO₂ content and a minimum number of impurities, its manufacturers use a wet enrichment method that includes washing, scrubbing, gravity, magnetic separation and flotation operations. This technology avoids dust formation during grinding and the pollution of the atmosphere, causing silicosis, so quartzite is moistened to 2–3%. For this reason, the use of wet quartzite for the preparation of the lining of tiger induction furnaces requires additional drying to a humidity of 0.3%, with the further production of tridymite and cristobalite phases [15–18].

The main supplier of quartzite is Pervoural Dinas Plant, which, in accordance with the technical conditions (TC 1511-022-00190495-2003) [46], sells it either with a humidity of less than 0.3% in special packaging or of 3% in ordinary bags. The supply of quartzite with a humidity of 3% implies the use of technology at the enterprise itself to remove excess moisture from the raw material, with a temperature treatment of around 900 °C.

Many businesses buy quartzite with a humidity of 3% and use it to remove excess moisture, with the following temperature mode: heating to a range of 800–900 °C and subsequent exposure for 8–10 h using stainless-steel packaging. This technology allows one to remove the bound moisture and obtain, after sintering in a newly made acidic lining, in a sintered layer, a tridyte phase. Figure 4 presents a sample embossed lining that has withstood 300 smelts from the middle of the kiln, smelting synthetic cast iron at melting temperatures not exceeding 1450 °C. It clearly traces the phases of the quartzite formed during the furnace operation.

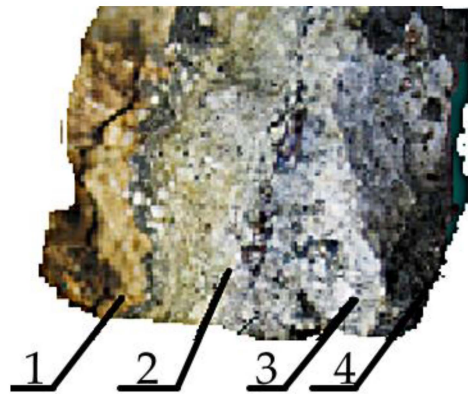


Figure 4. Sample embossed lining (photo taken at the moment of embossing in the furnace, during the production process): 1—Loose layer consisting of quartzite and boric acid; 2—Intermediate, half-baked layer consisting of quartzite and tridymite; 3—Sintered layer consisting of tridymite and a small amount of glazed phase; 4—Coated layer.

With optimal heating modes and sufficient quantities of mineral impurities (those currently used as mineralizers are CaO, FeO, MpO and substances containing them), the thermal structural transformations of quartz grains flow according to the following scheme: α -quartz \Leftrightarrow (573 °C) β -quartz \Leftrightarrow (870 °C) β -tridymite \Leftrightarrow (1470 °C) β -cristobalite.

Mineralizers play the role of the embryo centers of the new phase—cristobalite. At the same time, the concentration of impurities plays a decisive role: cristobalization occurs regardless of the grit of the samples when the concentration of mineralizers is in the range from 0.05% to 6%, and the conversion of quartz to cristobalite does not occur when the concentration of mineralizers is reduced to a threshold of 0.01% [47,48]. However, the formation of these phases depends not only on the chemical purity of the quartzite and the mineralizers used but also on the number of structural impurities and volatile components, the main ones being water (up to 92%) and carbon dioxide (up to 8%) [19] in trace amounts as various hydrogen-containing groupings [20–25]. Water changes in the silica matrix are among the reasons for its structural transformation under high-temperature conditions. The degree of crystallization of quartzite depends on many factors, including the number and composition of the GLI itself [26–28]. When exposed to high temperatures, silica is hydroxylated (CH group is converted to COH) with the breakdown of siloxane bonds (for Si-O-Si groups) and dehydroxylation, including the heating process, resulting in the hydroxyl group (OH) being released by the formation of a water molecule, which leads to the restructuring and reordering of the structure [29–32].

Water is present in several species. Physical moisture, i.e., water, is not part of the chemical composition of quartzite and is differently related to solid particles. Most of this water is located between the solids, mechanically filling the free space. The next type is mechanically bound water, which is weakly or almost not held by particulate matter and is easily removed when drying. This leads to the convergence of solids and the appearance of shrinkage. Film moisture formed around each solid particle the thinnest shell in a few dozen molecular layers. This water, due to the physical interaction, is firmly held by solid particles and is difficult to remove when drying. The process of removing it also causes particle convergence, but compared to the mechanically bound process, it is quite negligible at temperatures of 940–950 °C [33–36]. In addition, there are hydroxyl groups in quartzite in the composition of fine, water-containing mineral inclusions, the number of which depends on the content of molecular water, and point defects in the form of groupings of Al-OH, which begin to break down at 600 °C and are completely removed at 1100 °C. Its removal does not cause shrinkage [37,38].

The use of temperature-melting modes above 1450 °C requires the use of a higher temperature phase of quartzite, which is cristobalite.

This work includes studies of the influence of moisture in quartzite on the formation of its phases. The moisture was removed by drying the samples of the original quartzite at temperatures of 200 and 800 °C for 1 h and further cooling each sample to room temperature. These quartzite specimens were then exposed to temperatures of 200, 600, 870, 1000, 1470 and 1550 °C. The heating temperatures used in the experiment correspond to the sintering modes of the newly manufactured lining. As a result of the work carried out, conditions have been established for removing moisture from the original Pervoural quartzite, allowing one, during its further use, to obtain a phase of cristobalite. In the future, these studies will make it possible to develop a technology for manufacturing a high-temperature lining for an industrial-frequency induction crucible smelter; it provides high durability and improves the efficiency of the kiln itself and the production of castings in general.

2.2. Description of the Field Experiment

The study was carried out for the Pervoural quartzite of the brand PKMVI-3B, with a humidity of 3.5%, supplied by JSC “DINUR” under the technical conditions TC 1511-022-00190495-2003. According to the supplier, the finished product mainly contains quartz, but it also includes impurities of chalcedons, carbonates, opals and clay minerals, with low concentrations of iron oxides and a high dispersion. However, according to the TC, the company guarantees the chemical composition, as presented in Table 1 (the content of the remaining impurities is not given). In addition, the following grain composition is guaranteed, in mass fractions:

- The remainder is not grid 2, including 6–15;
- The balance on the grid is 3.2, not more than 5;
- Pass through the grid 05, including 50–59;
- Pass through grid 01-31-41.

Chemical analysis was carried out using the fundamental parameters for the X-ray fluorescence spectrometer Shimadzu XRF-1800 (Figure 5c). The device is equipped with collimators and a built-in digital camera, and the rotation speed of the sample was 60 rev/min.

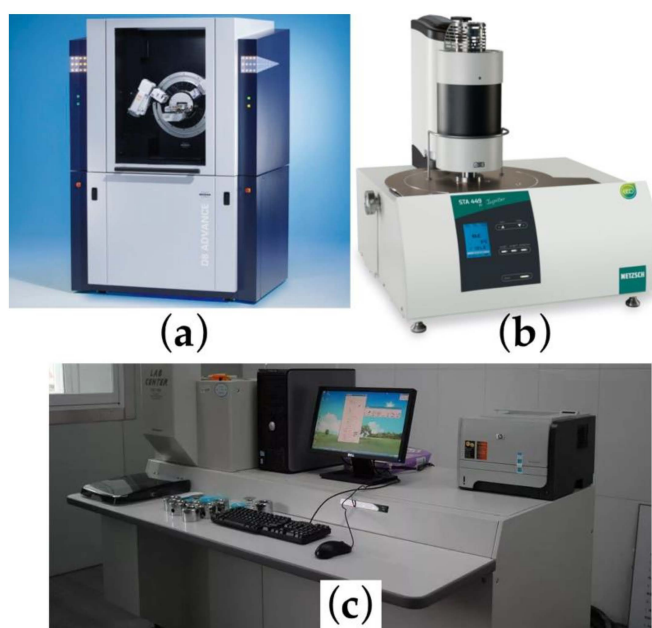


Figure 5. Equipment and research material: (a)—BRUKER D8 ADVANCE diffractometer; (b)—STA 449 F1 Jupiter derivative; (c)—Shimadzu XRF-1800 X-ray fluorescent wave-dispersion spectrometer.

The X-ray diffraction method was used to study the phase composition using the BRUKER D8 ADVANCE diffractometer, equipped with a Bragg–Brentano focus and an HTK

16 high-temperature chamber. A copper-anode X-ray tube was used, and the diffraction spectrum was recorded by the VANTEC-1 high-speed positional detector. The shooting took place at the angles of $2\Theta = 10\text{--}90$ in increments of 0.007, and the shooting time was 1 h (Figure 5a).

The thermal analysis of quartzite was carried out using STA 449 F1 Jupiter (NETZSCH, Selb, Germany) (Figure 5b).

2.3. Experimental Research Methodology

The definition of the chemical composition showed that the SiO_2 quantity was 96.84% instead of 97.5%, that of Al_2O_3 was 0.882 instead of 1.1%, that of Fe_2O_3 was 1.03% larger than declared and the amount of unspecified impurities was 1.149%.

The results of the analysis are shown in Table 3.

Table 3. Chemical composition of quartzite brand PKMVI-3.

Chemical Composition of PKMVI-3B Quartzite	Content (%)										
	SiO_2	Al_2O_3	CaO	MgO	TiO_2	Fe_2O_3	P_2O_5	MnO	CaO	Na_2O	K_2O
On Technical Condition	97.5	1.1	-	-	-	0.6	-	-	-	-	-
Spectrometer of dried sample at 200 °C	96.84	0.882	0.099	0.029	0.265	1.03	0.017	0.041	0.099	0.125	0.474

Then, using the derivative device STA 449 F1 Jupiter, changes in the mass of the quartzite during heating were determined (Figure 6).

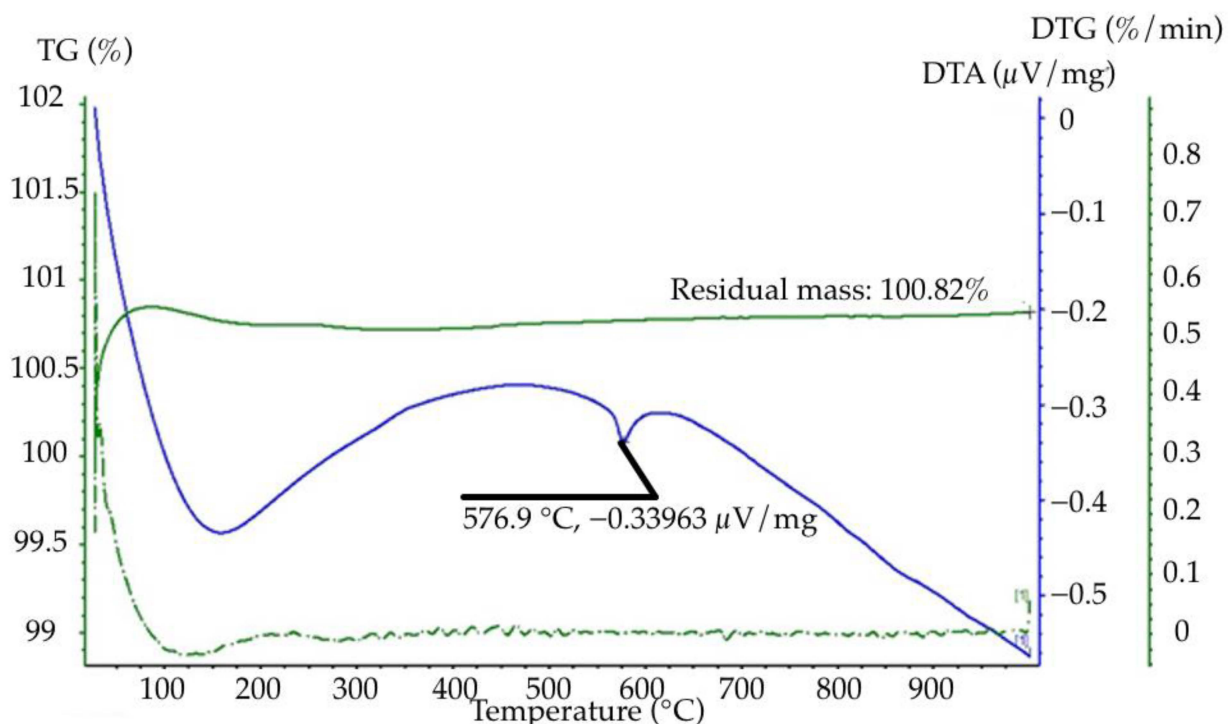


Figure 6. Derivative of a quartzite heated to 1000 °C: DTA-Ich curve from temperature; TG-Thermogram curve showing mass reduction; DTG-Thermogram curve indicating mass increase, which may occur due to the oxidation process.

There are two endothermic effects on the DTA curve. The first endoeffect at 170 °C refers to the loss of adsorbed (physically bound) water. In a study by Bas'yas devoted to the drying of quartzite powders for induction furnace lining, it was noted that weight

loss ceased after reaching a temperature of 105–110 °C. The second endoeffect at a temperature of 570 °C, passing without a loss of mass of the sample, refers to polymorphic transformation leading to the transformation of alpha-quartz phases into beta-quartz. It is accompanied by the beginning of the process of breaking point defects in the form of Al-OH clusters. From a temperature of 620–630 °C, no mass changes associated with water removal were detected.

The BRUKER D8 ADVANCE diffractometer was used to study the phase transformations of the moisture state in quartzite. Diffractograms were removed at temperatures of 200 and 800 °C, characterizing phase changes during moisture removal and subsequent cooling, and then during the heating used to sinter the lining. Figures 7 and 8 show the diffractograms of the quartzite in which the moisture was removed at 200 and 800 °C, respectively.

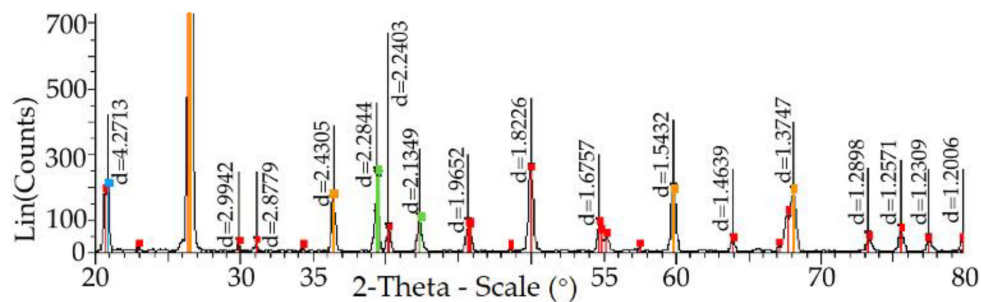


Figure 7. Diffractogram of the structure of a quartzite dried at 200 °C and cooled to 25 °C.

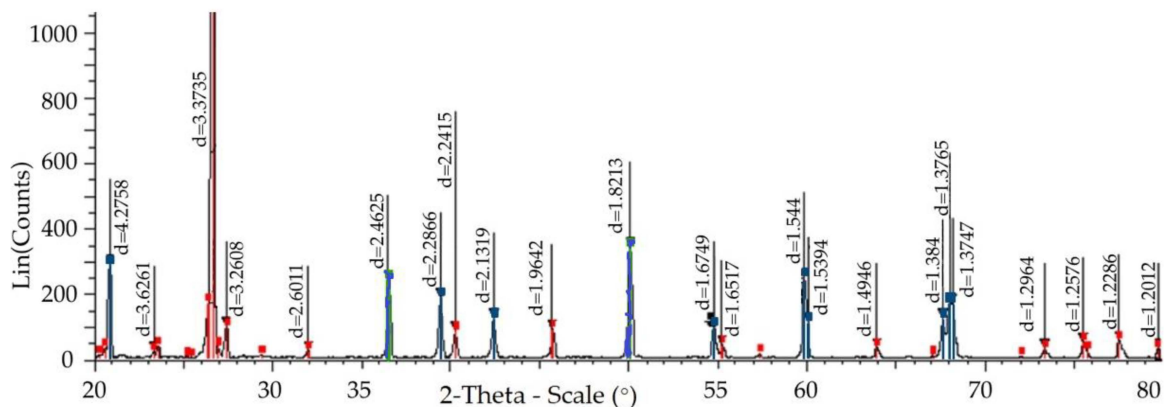


Figure 8. Quartzite diffractogram, taken at 30 °C.

The first stage involved examining quartzite that was dried at 200 °C and cooled to 25 °C.

The diffractogram in Figure 7 provides information on the parameters of the structure of quartzite dried at 200 °C and cooled to 25 °C. The lattice consists of four varieties of elemental quartzite cells, which are marked with different colors (blue, green, orange and red) in Figures 7 and 8.

In the second stage, a study was conducted on a sample of quartzite, which was rolled at 800 °C and cooled to 30 °C. The quartzite diffractogram, taken at 800 °C and cooled to 30 °C, is shown in Figure 8. It shows that the lattice structure consists of two elementary cells.

The interpretation of the result of the study of changes in the structure of the quartzite was carried out by the program of the device, which has a databank, in the form of cards of elementary cells with their characteristics and the subsequent determination of the average characteristics of the parameters of quartzite. Details of the calculation technology for the quartzite diffractogram removed at 870 °C are provided below (Figure 9).

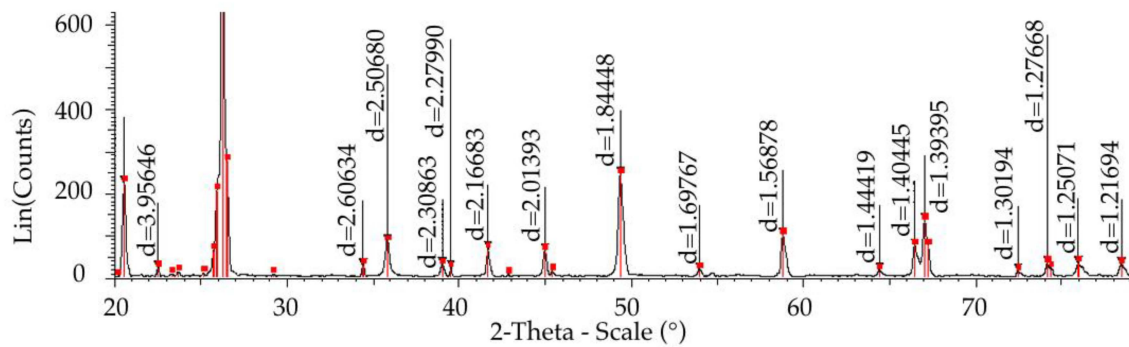


Figure 9. Quartzite diffractogram, taken at 879 °C, characterizing the appearance of cristobalite with $z = 7.16 \text{ \AA}$.

Then, the total number of crystalline phases was determined, the content of which is at least 5% and is taken by 100%. The fraction of each crystalline phase was then determined, and its mean interdust distance was calculated. Then, d_{avg} was defined for the whole grid.

As a result, the following results of the characteristics of the parameters of quartzite, subjected to temperature conditions of the sintering of the lining, were obtained, and the dependence of phase formation on the condition of moisture in the quartzite was identified (Table 4).

Table 4. Quartzite crystal lattice parameters for different moisture states.

Lattice Parameter	Temperature (°C)								
	25 Crude	200/800	25/30 Dry	200	600	870	1000	1470	1550
d_{avg} (Å)	2.676	2.908/ 3.012	2.814/ 2.7574	2.8340/ 2.9012	2.7913/ 3.0066	2.9277/ 3.0545	2.9796/ 3.1048	3.0384/ 3.156	3.2619/ 3.2156
V_{avg} (Å ³)	115.4	116.35/ 129.85	119.1/ 114.83	116.55/ 115.41	117.47/ 647.47	125.86/ 1653.02	124.06/ 1722.83	124.04/ 1742.69	143.65/ 1606.96
D_{avg} (g/cm ³)	2.590	2.552/ 2.249	2.5971/ 2.601	2.552/ 2.592	2.333/ 2.502	2.292/ 2.2685	2.291/ 2.266	2.229/ 2.265	2.227/ 2.258
M_{avg} (g/mol)	60.08	60.08/ 51.01	60.08/ 60.08	60.08/ 60.08	55.16/ 60.08	53.91/ 58.38	53.66/ 58.63	53.66/ 58.79	54.41/ 58.79

In Table 4, the numerators represent the values for the quartzite in which the moisture is removed at 200 °C, and the denominators represent these values at 800 °C. d_{avg} is the average interglobular distance, D_{avg} is the average density, V_{avg} is the average volume and M_{avg} is the average molecular mass of the lattice.

3. Results and Discussion

A quartzite roll at 800–900 °C results in the removal of bound (molecular) water and an increase of 3.5% in the mean intersex distance d_{avg} and of 1.6% in D_{avg} , along with an 11.8% decrease in V_{avg} and a 15.9% decrease in M_{avg} . It consists of cells characterized by the cards 00-012-0708 and 01-071-0911 with $M = 52.87 \text{ g/mole}$ and the appearance of cristobalite (card 01-085-0621). The lattice has the following characteristics: average intergloss distance $d_{\text{avg}} = 3.012 \text{ \AA}$, volume $V_{\text{avg}} = 129.853 \text{ \AA}^3$, density $D_{\text{avg}} = 2.249 \text{ g/cm}^3$ and molecular mass $M_{\text{avg}} = 51.01 \text{ g/mol}$.

After cooling to 30 °C, the lattice parameters changed, containing only cells 00-012-0708 and 01-083-2187: $d_{\text{avg}} = 2.7574 \text{ \AA}$, volume $V_{\text{avg}} = 114.83 \text{ \AA}^3$, density $D_{\text{avg}} = 2.601 \text{ g/cm}^3$ and molecular mass $M_{\text{avg}} = 60 \text{ g/mol}$.

The cooling of quartzite is necessary for the further mixing with boric acid (production of lining mass), the packing of the kiln and the sintering of the resulting lining on a special schedule. Sintering is carried out using temperatures from 25 to 30 °C (workshop air temperature) and 1550 °C. During the cooling process, the mixing process and the full

use of dried quartzite, it gains little moisture. For this reason, at a temperature of 200 °C, the parameters of the lattice change, so d_{avg} increases by 9.1% and V_{avg} increases by 0.5%, whereas D_{avg} decreases by 0.4%, which is also reflected in the derivative as a slight change in mass.

At 600 °C, no mass change is observed, but the Al-OH groupings begin to break down, and a polymorphic transformation occurs, which leads to the emergence of an elementary cell of tridymite card 01-071-0032, resulting in a five-fold increase in V_{avg} .

Heating up to 870 °C is characterized by the further destruction of Al-OH clusters and the appearance of new elementary cells; tridymite 00-018-1170 begins to break down Al-OH, and the V_{avg} increases by 14 times, d_{avg} increases by 10.7%, D_{avg} decreases by 2.8% and M_{avg} decreases by 6.2%.

At 1000 °C, the dissociation of the Al-OH groupings continues with the formation of H₂, increasing the proportion of elementary tridymite cells and increasing the value of V_{avg} by 15 times, d_{avg} by 12.5%, D_{avg} by 2.9% and M_{avg} by 6.2%.

Heating up to 1470 °C results in the final dissociation of the Al-OH groupings and the following changes in lattice parameters: the value V_{avg} is retained, d_{avg} is increased by 14.5% and D_{avg} and M_{avg} are retained.

A temperature of 1550 °C is characterized by the appearance of elementary cells of cristobalite (card 01-085-0621) and the following changes in grid parameters: d_{avg} increases by 16.6% and V_{avg} by 14 times.

The next option is to remove moisture and GLI from the original quartzite PKMI-3V, which involves drying it at 200 °C and then cooling it to ambient temperature (25–30 °C). During drying, the maximum free water is removed, the grid consists of cells characterized by cards 00-012-0708, 01-070-7344, 00-005-0490 and 01-083-2187, and the parameters of the grid itself acquire the following values: $d_{avg} = 2.908 \text{ \AA}$, $V_{avg} = 116.35 \text{ \AA}^3$, $D_{avg} = 2.552 \text{ g/cm}^3$ and $M_{avg} = 60.68 \text{ g/mol}$.

When cooled, a small amount of moisture is returned, and the parameters of the grating (compared to dried) are as follows: d_{avg} decreases by 3.3%; V_{avg} and d_{avg} increase by 2.4 and 1.8%.

Heating up to 200 °C is accompanied by the removal of moisture produced during the cooling, the preparation of the lining and the lining of the furnace, changes in the share of elemental cells formed during cooling and changes in the parameters of the grid (compared to dried and chilled), as follows: d_{avg} increases by 0.7%, V_{avg} decreases by 2.1%, D_{avg} decreases by 1.8% = 2.552 g/cm^3 and M_{avg} does not change.

At 600 °C, the mass does not change, the process of breaking Al-OH groups begins, the structure consists of two varieties of elementary cells with cards 01-083-2187 and 01-071-0911 with $M = 52.87 \text{ g/mole}$ and the parameters of the grid change are as follows: d_{avg} decreases by 0.8%, V_{avg} decreases by 3.8%, D_{avg} decreases by 10.1% = 2.552 g/cm^3 and M_{avg} decreases by 8.1%.

Heating up to 870 °C is accompanied by the further destruction of Al-OH groups, the emergence of the elementary cell of cristobalite, with the card 00-011-0695, and changes in the parameters of the grid: d_{avg} increases by 4.0%, V_{avg} decreases by 5.6%, D_{avg} decreases by 10.7% = 2.552 g/cm^3 and M_{avg} decreases by 10.3%.

The temperature of 1000 °C contributes to the continuation of the dissociation process of the Al-OH groupings with the formation of H₂ and the following changes in grid parameters: d_{avg} increases by 5.9%, V_{avg} increases by 4.1%, D_{avg} decreases by 11.8% and M_{avg} by 10.7%.

At 1470 °C, the dissociation process of Al-OH groups ended and, among the parameters of the lattice, changed the number of d_{avg} , which increased by 8.0%.

Heating up to 1550 °C results in another elemental cell, the crystallite 00-002-0278, and significant changes in lattice parameters: d_{avg} increases by 15.9%, the value of V_{avg} increases by 20.6%, D_{avg} remains at 1470 °C and M_{avg} decreases by 9.5%.

All the changes were compared with dry quartzite after drying at temperatures of 200/800 °C. The values of d_{avg} , V_{avg} , D_{avg} and M_{avg} were determined on the basis of the

obtained data for the interdimensional distances of each diffractogram and the cards of elementary cells used by the instrument program.

4. Conclusions

Studies have found that the state of moisture and GLI in quartzite, which is detected after its temperature treatment during drying and further exposure to temperature melting, has a great influence on the process of phase formation (tridymite and cristobalite).

It has been established that impurities detected by the X-ray fluorescent wave-dispersion spectrometer Shimadzu XRF-1800 in the amount of 1.149% are not mineralizers; however, when using a traditional proclimator at 800 °C, the phase transformation of the quartzite remains unchanged. At 600 °C, a polymorphic transformation occurs, which results in the emergence of a tridymite elementary cell, and the cells of the cristobalite appear only at 1550 °C.

Studies using the derivative STA 449 F1 Jupiter showed that free water is removed from the quartzite at temperatures of 170–200 °C. This is characterized by the first endoefficiency derivative and refers to the loss of adsorbed (physically bound) water. The second endoeffect is observed at a temperature of 570 °C and relates to polymorphic transformation leading to alpha-quartz phase formation in beta-quartz. It is accompanied by the beginning of the process of removing chemically bound water and is not accompanied by a change in mass.

It has thus been established that moisture plays the role of a mineralizer, and its condition influences the formation of specific phases. This assumption was made in a previous study [39]. Temperature treatment at 800 °C results in the complete removal of free water and a significant amount of chemically bonded moisture, including GWG, resulting in the tridymization of the quartzite.

Drying at 200 °C results only in the removal of free water and contributes to the process of crystallization. Cristobalite begins to appear at 870 °C, and the tridymite phase is not detected, even at 1550 °C.

It has been determined that tridymite, in the temperature range of 1000–1550 °C (this is the working temperature for the smelting of synthetic cast iron from metal filling consisting of up to 90% steel scrap) allows for volume changes at a limit of 9% and cristobalite at a limit of 15%.

Thus, the lining in which the quartzite contains only chemically bonded moisture, after the sintering of the lining, is converted to cristobalite and provides a more stable exposure to sudden temperature changes. This allows for the application of the melting temperatures necessary for the metal filling of up to 90% of steel scrap, which increases the efficiency of the melting furnace and the production of castings in general.

In the future, it is advisable to carry out studies on the quartzite of other deposits to determine the possibility of their use as the base material of the lining of various induction furnaces. This is due to the increased requirement for liner materials.

Author Contributions: Conceptualization, V.A.K., A.I.C. and V.S.T.; Data curation, V.A.K., A.I.C., V.V.K., V.S.T., S.O.K., V.V.B., A.A.B. and R.B.S.; Formal analysis, V.A.K., A.I.C., V.V.K., V.S.T., S.O.K., V.V.B., A.A.B. and V.V.T.; Investigation, V.A.K., A.I.C., V.V.K., V.S.T., S.O.K., K.A.B., V.V.B., A.A.B. and R.B.S.; Methodology, V.A.K., V.V.K., K.A.B. and V.V.T.; Project administration, V.A.K., A.I.C. and V.S.T.; Resources, V.A.K. and S.O.K.; Supervision, V.A.K., A.I.C. and V.S.T.; Validation, A.I.C., V.V.K., V.S.T., S.O.K., K.A.B., R.B.S. and V.V.T.; Visualization, V.V.K., R.B.S. and V.V.T.; Writing—original draft, V.A.K., A.I.C., V.V.K., V.S.T., K.A.B., R.B.S., V.V.B., A.A.B. and V.V.T.; Writing—review & editing, V.A.K., A.I.C., V.V.K., V.S.T., S.O.K., K.A.B., R.B.S., V.V.B., A.A.B. and V.V.T. All authors have read and agreed to the published version of the manuscript.

Funding: This research received no external funding.

Institutional Review Board Statement: Not applicable.

Informed Consent Statement: Not applicable.

Data Availability Statement: Not applicable.

Conflicts of Interest: The authors declare no conflict of interest.

References

1. Legemza, J.; Findorák, R.; Bul'ko, B.; Briančin, J. New Approach in Research of Quartzes and Quartzites for Ferroalloys and Silicon Production. *Metal* **2021**, *11*, 670. [CrossRef]
2. Mirzaev, B.; Bozarova, M. Status and Prospects of Foundry Production in Russia. In Proceedings of the Innovative Approaches in Modern Science, Materials of the CVIII International Scientific and Practical Conference, Moscow, Russia, 21 December 2021; pp. 92–95.
3. Adetunji, O.; Ojo, S.S.; Oyetunji, A.; Itua, N.; Adetunji, O.; Ojo, S.S.; Oyetunji, A.; Itua, N. Melting Time Prediction Model for Induction Furnace Melting Using Specific Thermal Consumption from Material Charge Approach. *J. Miner. Mater. Charact. Eng.* **2020**, *9*, 61–74. [CrossRef]
4. Sassa, V.S. *Lining of Induction Melting Furnaces and Mixers*; Energoatomizdat: Moscow, Russia, 1983.
5. Kostyukova, A.P. Institutional Method as the Basis for Monitoring the Induction Melting Furnace. *Adv. Mod. Sci.* **2017**, *4*, 19–23.
6. Druzhevsky, M.A.; Subdue, B. Lining of Induction Melting Furnaces with Materials Based on Quartzite. *Liteynoye Proizv.* **2010**, *4*, 33–38.
7. Futas, P.; Pribulova, A.; Petrik, J.; Pokusova, M.; Junakova, A. The Study of Synthetic Cast Iron Quality Made from Steel Scrap. In Proceedings of the 18th International Multidisciplinary Scientific GeoConference SGEM 2018, Vienna, Austria, 3–7 December 2018; pp. 321–329.
8. Nelub, V.; Gantimurov, A.; Borodulin, A. Economic Analysis of Data Protection in Systems with Complex Architecture Using Neural Network Methods. *Econ. Ann.* **2020**, *185*, 178–188. [CrossRef]
9. Edalati, K.; Akhlaghi, F.; Nili-Ahmadabadi, M. Influence of SiC and FeSi Addition on the Characteristics of Gray Cast Iron Melts Poured at Different Temperatures. *J. Mater. Process. Technol.* **2005**, *160*, 183–187. [CrossRef]
10. Zavertkin, A.S. Development of the Composition of the Lining of Induction Furnaces from Pervouralsk Quartzite and the Practice of Its Application. *Proc. Kola Sci. Cent. Russ. Acad. Sci.* **2015**, *44*, 532–534.
11. Nelyub, V.A. The Effect of Copper and Zinc Coatings on the Properties of Carbon Fibers and Composites Based on Them. *Polym. Sci. Ser. D* **2021**, *14*, 260–264. [CrossRef]
12. Fireproof Mass for Printed Lining. Patent 2011647 from 30.04.1994. Available online: https://i.moscow/patents/RU2011647C1_19940430 (accessed on 4 September 2022).
13. Silica Refractory Mass. Patent 2127234 from 25.04.1979. Available online: <https://patentdb.ru/patent/2127234> (accessed on 4 September 2022).
14. Volodichev, O.I. *Mineralogy, Petrology and Minerageny of Precambrian Complexes in Karelia*, 1st ed.; Karelian Research Centre Russian Academy of Sciences Institute of Geology: Petrozavodsk, Russia, 2007; pp. 1–124.
15. Kukartsev, V.A. Application of Pervouralsky Quartzite in Acid Lining for Induction Iron-Smelting Furnaces. *Liteyshchik Russ.* **2012**, *2*, 35–37.
16. Stoyanova, M.V.; Novikov, A.D.; Borodulin, A.S. Evaluation Construction Made of Polymer Composite Materials by Molding Using Reusable Flexible Punches Production Profitability. *IOP Conf. Ser. Mater. Sci. Eng.* **2020**, *934*, 012068. [CrossRef]
17. Ananiev, Y.S.; Ananyeva, L.G.; Dolgov, I.V.; Korobeinikov, A.F.; Korovkin, M.V. Search, Evaluation and Enrichment of Quartz Raw Materials for High Technologies. *Bull. Tomsk Polytech. Univ. Geores. Eng.* **2001**, *304*, 123–130.
18. Rajan, H.; Uchida, H.; Bryan, D.L.; Swaminathan, R.; Downs, R.T.; Hall-Wallace, M. Building the American Mineralogist Crystal Structure Database: A Recipe for Construction of a Small Internet Database. *Geoinform. Data Knowl. Geol. Soc. Am. Spec. Pap.* **2006**, *397*, 73–80. [CrossRef]
19. Kosenko, N.F.; Smirnova, M.A. Mechanostimulated Polymorphic Transitions of Quartz. *Refract. Tech. Ceram.* **2012**, *7*, 7–13.
20. Riposan, I.; Chisamera, M.; Stan, S. Enhanced Quality in Electric Melt Grey Cast Irons. *ISIJ Int.* **2013**, *53*, 1683–1695. [CrossRef]
21. Kukartsev, V.A.; Abkaryan, A.K.; Temnykh, V.I.; Kukartsev, V.V.; Tynchenko, V.S.; Kukartsev, A.V. The Changes of Pervouralsky Quartzite Crystal Lattice under Heating from up 25 to 600 °C. *Novyye Ogneup.* **2021**, *1*, 34–39. [CrossRef]
22. Hanagiri, S.; Matsui, T.; Shimo, A.; Aso, S.; Inuzuka, T.; Matsuda, T.; Sakaki, S.; Nakagawa, H. Recent Improvement of Recycling Technology for Refractories. *Shinmittetsu Giho* **2008**, *388*, 93–98.
23. Kukartsev, V.A.; Kukartsev, V.V.; Kukartsev, A.V. Effect of the Temperature Treatment of Quartzite on the Lining Resistance of Commercial-Frequency Induction Crucible Furnaces. *Refract. Ind. Ceram.* **2018**, *59*, 252–256. [CrossRef]
24. Downs, R.T.; Hall-Wallace, M. The American Mineralogist Crystal Structure Database. *Am. Mineral.* **2003**, *88*, 247–250.
25. Ringdalen, E. Changes in Quartz During Heating and the Possible Effects on Si Production. *JOM* **2015**, *67*, 484–492. [CrossRef]
26. Pryanishnikov, V.P. *Silica System*; Stroyizdat: Leningrad, Russia, 1971; Volume 238.
27. Novakovic, R.; Radic, S.M.; Ristic, M.M. Kinetics and Mechanism of Quartz-Tridymite Transformation. *Nterceram Interceram* **1986**, *35*, 29–30.
28. Breneman, R.C.; Halloran, J.W. Kinetics of Cristobalite Formation in Sintered Silica. *J. Am. Ceram. Soc.* **2014**, *97*, 2272–2278. [CrossRef]
29. Shchiptsov, V.V.; Perepelitsyn, V.A.; Grishenkov, E.E.; Enenko, V.P.; Zavertkin, A.S. Pervoural'skii and Karel'skii Quartzites for the Lining of Crucible-Type Induction Furnaces. *Refract. Ind. Ceram.* **2003**, *44*, 67–74. [CrossRef]

30. Nikiforova, E.M.; Eromasov, R.G.; Simonova, N.S.; Vasilyeva, M.N.; Taskin, V.Y. Phase Transformations in the Siliceous Rocks-Mineralizer System. *Mod. Probl. Sci. Educ.* **2012**, *1*, 218–219.
31. Li, W.; Xu, C.; Xie, A.; Chen, K.; Yang, Y.; Liu, L.; Zhu, S. Microstructure Study of Phase Transformation of Quartz in Potassium Silicate Glass at 900 °C and 1000 °C. *Crystals* **2021**, *11*, 1481. [[CrossRef](#)]
32. Kukartsev, V.A.; Kukartsev, V.V.; Tynchenko, V.S.; Bukhtoyarov, V.V.; Tynchenko, V.V.; Sergienko, R.B.; Bashmur, K.A.; Lysyannikov, A.V. The Technology of Using Liquid Glass Mixture Waste for Reducing the Harmful Environmental Impact. *Materials* **2022**, *15*, 1220. [[CrossRef](#)] [[PubMed](#)]
33. Nelyub, V.A.; Fedorov, S.Y.; Malysheva, G.V.; Berlin, A.A. Properties of Carbon Fibers after Applying Metal Coatings on Them by Magnetron Sputtering Technology. *Fibre Chem.* **2021**, *53*, 252–257. [[CrossRef](#)]
34. Wahl, F.M.; Grim, R.E.; Graf, R.B. Phase Transformations in Silica as Examined by Continuous X-ray Diffraction | American Mineralogist | GeoScienceWorld. *Am. Mineral. J. Earth Planet. Mater.* **1961**, *46*, 196–208.
35. Benarieb, I.; Duyunova, V.A.; Oglodkov, M.S.; Puchkov, Y.A.; Pakhomkin, S.I. Quench Factor Analysis for Predicting Precipitation Hardening of Sheets from Aluminum Alloy V-1341 of the Al–Mg–Si System. *Met. Sci. Heat Treat.* **2022**, *63*, 583–589. [[CrossRef](#)]
36. Voronin, A.S.; Fadeev, Y.V.; Makeev, M.O.; Mikhalev, P.A.; Osipkov, A.S.; Provatorov, A.S.; Ryzhenko, D.S.; Yurkov, G.Y.; Simunin, M.M.; Karpova, D.V.; et al. Low Cost Embedded Copper Mesh Based on Cracked Template for Highly Durability Transparent EMI Shielding Films. *Materials* **2022**, *15*, 1449. [[CrossRef](#)]
37. Kukartsev, V.A.; Cherepanov, A.I.; Kukartsev, V.V.; Tynchenko, V.S.; Bukhtoyarov, V.V.; Popov, A.M.; Sergienko, R.B.; Tynchenko, S.V. X-ray Diffraction Phase Analysis of Changes in the Lattice of Pervouralsk Quartzite upon Heating. *Minerals* **2022**, *12*, 233. [[CrossRef](#)]
38. Platonov, B.P.; Akimenko, A.D.; Bagutskaya, S.M. *Induction Furnaces for Cast Iron Melting*; Mashinostroyeniye: Moscow, Russia, 1976.
39. Satr, P. New Refractory Technology for Melting Cast Iron Alloys and Alloy Steel in Induction Furnaces. *Liteyshchik Russ.* **2019**, *1*, 11–15.
40. Kukartsev, V. Increase in the Life of the Industrial Induction Crucible Furnace at Temperatures above 1550 C. *Technol. Mech. Eng.* **2014**, *1*, 5–6.
41. Zavertkin, A.S. Effect of Quartzite Heat Treatment on Induction Furnace Lining Failure Mechanism. *Refract. Ind. Ceram.* **2019**, *60*, 67–70. [[CrossRef](#)]
42. Kukartsev, V.A.; Trunova, A.I.; Kukartsev, A.V. Thermal Analysis of Quartzite Used to Line a Crucible-Equipped Industrial-Frequency Induction Furnace. *Refract. Ind. Ceram.* **2014**, *55*, 220–222. [[CrossRef](#)]
43. He, J.; Jusnes, K.F.; Tangstad, M. Phase Transformation in Quartz at Elevated Temperatures. *Asp. Min. Miner. Sci.* **2021**, *6*, 691–699. [[CrossRef](#)]
44. Shakirov, K.M.; Sokolov, G.S.; Nelyub, V.A. Research of Transversal Properties of Winding Basalt Plastics Based on Basalt Fiber with Experimental Lubricants. *J. Phys. Conf. Ser.* **2021**, *1990*, 012044. [[CrossRef](#)]
45. Orlov, M.A.; Nelyub, V.A.; Kalinnikov, A.N.; Borodulin, A.S. Modeling Basalt Fibers Wetting Processes Used in the Basalt Rebar Production. *J. Phys. Conf. Ser.* **2021**, *1990*, 012042. [[CrossRef](#)]
46. Quartzite Ground Pervoural Dynasty Plant for Induction Furnace Crucifixes. TC 14-8-542-87 from 01.01.1988. Available online: <https://www.standards.ru/document/3230296.aspx> (accessed on 11 September 2022).
47. Skamnitskaya, L.S.; Svetova, E.N.; Shanina, S.N. The Effect of Fluid Inclusions on the Vein Quartz Grade. *Obogashchenie Rud* **2019**, *2019*, 20–26. [[CrossRef](#)]
48. Zavertkin, A.S. Development of a Lining Made from Karelian Quartzites for Crucible Induction Furnaces. *Refract. Ind. Ceram.* **2010**, *50*, 400–405. [[CrossRef](#)]